Available online at www.sciencedirect.com
SCIENCE DIRECT®
Journal of Organometallic Chemistry 690 (2005) 1356–1365
Journal of Organometallic Chemistry
www.elsevier.com/locate/jorganchem

Density functional study on the role of electron donors in propylene polymerization using Ziegler–Natta catalyst

Sami Mukhopadhyay [a,*], Sudhir A. Kulkarni [a], Sumit Bhaduri [b]

[a] VLife Sciences Technologies Private Limited, 1 – Akshay, # 50, Anand Park, Aundh, Pune 411 007, India
[b] Reliance Industries Limited, Swastik Mill Compound, V.N. Purav Marg, Chembur, Mumbai 400 071, India

Received 2 September 2004; accepted 1 December 2004
Available online 8 January 2005

Abstract

The role of electron donors in propylene polymerization using Ziegler–Natta model catalyst $[TiCl_2CH_3]^+$ has been investigated using density functional calculations at B3LYP/6-31G* level. Methyl benzoate (MBz) and *para*-methoxy methyl benzoate (*p*-OMe-MBz) are the electron donors considered in this study. We have found two major roles of these electron donors that match well with the corresponding experimental results. First, for both the catalysts having different electron donors, the propylene insertion in Ti–CH_3 bond in *syn*-fashion rather than *anti*-fashion has lower activation barriers (E_{act}). This indicates that the regioselectivity of propylene insertion is maintained in the presence of the electron donors. Secondly, co-ordination of electron donors is found to increase the activation barriers of propylene insertion, which explains the experimentally observed drop in catalytic activity of $[TiCl_2Me]^+$ on adding electron donors.

Keywords: Density functional; Electron donors; Ziegler–Natta catalyst; Propylene insertion; Regioselectivity; Stereospecificity

1. Introduction

Polypropylene of high isotacticity is a versatile material with a conservative estimate of global production of 30 million tons in 2005 [1]. Most of the commercial catalysts used for polypropylene manufacture, are modifications and improvements of the original Ziegler–Natta (ZN) system. They consist of three components: $MgCl_2$ supported $TiCl_4$, trialkyl or dialkyl aluminum chloride and organic additives [2]. In the patent literature the organic additives are normally referred to as the electron donors. During the preparation of $MgCl_2$ supported $TiCl_4$, a mono- or diester is added and these are known as the internal electron donors. During polymerization, another additive usually another ester or ether is added, and these are referred to as the external electron donor. Specific combinations of internal and external electron donors have major influence on the activity of the catalyst, as well as the isotacticity of the resultant polypropylene. One such combination, most extensively used industrially, is ethyl benzoate and *p*-ethoxy ethylbenzoate as the internal and external electron donor, respectively.

There is spectroscopic and X-ray structural evidence to show that the electron donors can, and do co-ordinate to titanium and magnesium ions [3]. There is some evidence to suggest that electron donors deactivate the atactic catalytic sites [4]. It has also been proposed that co-ordination of electron donors to or near the catalytic sites increases the number of asymmetric active sites, i.e., isotactic sites [5]. These hypotheses are consistent with quantitative data that show that as the concentra-

* Corresponding author. Tel.: +912025886737; fax: +912025 886737.
E-mail addresses: samim@vlifesciences.com (S. Mukhopadhyay), sudhirk@vlifesciences.com (S.A. Kulkarni), sumit_bhaduri@ril.com (S. Bhaduri).

0022-328X/$ - see front matter © 2004 Elsevier B.V. All rights reserved.
doi:10.1016/j.jorganchem.2004.12.002

tion of electron donor increases, the isotacticity increases but the productivity or turnover number decreases. Apart from the benzoate esters, experimental data on the ability of other donors like phthalates and diethers on productivity and tacticity of ZN catalytic systems have also been reported [6i–k].

In recent years, DFT based theoretical calculations have proved to be useful for rationalizing a number of empirical observations on polymerization reactions using ZN catalysts [4a,b,6a–m,7]. Earlier, electronic structure studies on regioselective preferences of propylene insertion were reported using ab initio methods with $[TiCl_2Me]^+$ (Me═CH_3) as model catalyst [6c]. It was shown that the non-planarity of the transition state of propylene insertion in $[TiCl_2Me]^+$ makes one of the two stereo-specific *syn* insertion pathways substantially more favorable than the other. It was further analyzed in the same study that this tendency of a non-planar transition state may have more significance in determining stereo-specificity in the chain growth step of olefin polymerizations in $[RTiCl_2]^+$.

In a recent DFT based Car–Parrinello molecular dynamics(CPMD) study of $TiCl_4/MgCl_2$ ZN catalyst for isotactic propylene polymerization, Boero et al. showed the regioselective preference of propylene insertion in *syn*(1,2) fashion over *anti*(2,1) fashion in the Ti–alkyl bond [6d]. The enantioface selectivity of one of the *syn* faces of propylene was inferred from steric interactions and comparison of the corresponding activation barriers. This study considers the highly reactive Ti(IV) 5-fold coordinated center [6e] as the dominant catalytic species possessing high degree of stereoselectivity to select the appropriate propylene enantioface in the chain growth process [6d].

Using a similar theoretical model, Boero et al. [4b] studied the role of a typical internal electron donor like di-*n*-butyl phthalate in poisoning the active sites and deactivating the ZN catalyst. It is shown that such phthalate donors deactivate the catalyst by binding strongly to and thereby poisoning Ti centers such as the 6-coordinated Corradini one [6f–h] on the (1 1 0) $MgCl_2$ surface while leaving the 5-fold coordinated Ti sites unaffected. Ziegler and co-workers [6l] studied several models of active sites for solid $TiCl_4/MgCl_2$ ZN catalyst and proposed $TiCl_3$ based sites as relevant. Further, by QM(DFT)/MM studies [4a] they found that an external base like THF used in the $TiCl_4/MgCl_2$ ZN catalyzed ethylene polymerization mostly coordinates to the Al–alkyl monomer or a $TiCl_3$-based site causing poisoning of the active sites and catalyst deactivation.

Recently, using DFT studies we investigated the factors responsible for variation of activity in ZN catalyst for ethylene and propylene polymerization with different ligands such as the conventional chloride, chloroalkoxy, alkoxy and non-alkoxy types [7a,b]. The activation barriers for propylene insertion in the Ti–CH_3 bond was consistently lower for *syn*(1,2) insertion than for *anti*(2,1) for all the catalysts studied. This is in accordance with the general observation, that in propylene polymerization with commercial ZN catalysts, *syn*(1,2) insertion is the preferred mode [6c,d].

The present work is our next step in a systematic approach to explore the mechanistic aspects of propylene polymerization by ZN catalysts. More specifically, here we investigate the roles of ethyl benzoate and *p*-ethoxy ethyl benzoate as electron donors, in tuning regio- and stereoselective preferences of propylene polymerization. For computational simplicity we have modeled these two electron donors by methyl benzoate and *p*-methoxy methylbenzoate respectively, and the catalyst precursor by $[TiCl_2Me]^+$.

2. Methodology

Titanium in the present study is considered to be in +4 oxidation state. The active catalysts selected for this work are slight modifications of that originally suggested by Cossee [6n,o]. In the active catalysts, the electron donors, methyl benzoate (MBz) and *para*-methoxy methyl benzoate (*p*-OMe-MBz) are proposed to be coordinated to the titanium center of $[TiCl_2CH_3]^+$. Using this active catalyst and methyl benzoate and *p*-OMe methyl benzoate as internal additives, we have investigated stationary points on the potential energy surface (PES) of propylene polymerization. All the geometries have been obtained using hybrid density functional method B3LYP [8] (three parameter Becke's exchange energy functional along with correlation functional due to Lee, Yang and Parr). The basis set used is 6-31G*. The vibrational frequencies and zero point corrected energies (ZPE) of all the stationary points on the PES have been obtained (cf. Tables 1 and 2). All the calculations have been performed using ab initio program GAUSSIAN 98 [9].

3. Results and discussion

The optimized structures of all reactants, viz. propylene, $[TiCl_2Me]^+$, and electron donors MBz and *p*-OMe-MBz are displayed in Fig. 1. The optimized geometries of stationary points observed on the PES of propylene insertion in the active catalysts, i.e., $[MBz...TiCl_2CH_3]^+$ and $[p\text{-OMe-MBz}...TiCl_2CH_3]^+$, at B3LYP/6-31G* level are displayed in Figs. 2 and 4, respectively. The meaning of *syn* and *anti* terminology used throughout this work refers to the relative orientations of the methyl group of propylene with respect to the Ti–CH_3 bond. If both the methyl groups are on the same side then the structure is called *syn*, otherwise it is referred to as *anti*. It may be noted that the insertion of propylene in the

Table 1
Zero point energy (ZPE) corrected relative energies (kcal/mol) of stationary points on the PES of propylene insertion in Ti–CH_3 bond of $[MBz...TiCl_2CH_3]^+$ as active catalyst at B3LYP/6-31G* level[a] and the values in parentheses are relative energies (kcal/mol) obtained from single point calculations at B3LYP/ 6-311+G(d,p) level[b]

Structure	*E*(Complex)	*E*(TS)	E_{act}[c]	*E*(Product)
Syn-si	−3.55 (−2.03)	12.96 (14.18)	16.51 (16.21)	−19.05 (−18.18)
Syn-re	−3.28 (−1.85)	12.88 (14.28)	16.16 (16.13)	−17.89 (−17.10)
Anti-si	−4.01 (−2.46)	15.56 (16.88)	19.57 (19.34)	−18.31 (−17.50)
Anti-re	−3.97 (−2.24)	16.09 (17.22)	20.06 (19.46)	−18.62 (−17.70)

[a] Total ZPE corrected energies (electronic + ZPE in a.u.) of active catalysts and olefin are: $[MBz...TiCl_2CH_3]^+ = -2269.605274$; $C_3H_6 = -117.827460$. MBz = methyl benzoate internal additive. ZPEs used are without scaling.
[b] Single point energies (in a.u.) of active catalyst and olefin are: $[MBz...TiCl_2CH_3]^+ = -2270.030136$; $C_3H_6 = -117.945385$.
[c] E_{act} is insertion barrier in kcal/mol.

Table 2
Zero point energy (ZPE) corrected relative energies (kcal/mol) of stationary points on the PES of propylene insertion in Ti–CH_3 bond of $[p\text{-OMe-MBz}...TiCl_2CH_3]^+$ as active catalyst at B3LYP/6-31G* level[a]

Structure	*E*(Complex)	*E*(TS)	E_{act}[b]	*E*(Product)
Syn-si	−2.04	14.61	16.65	−18.60
Syn-re	−1.92	14.49	16.41	−17.54
Anti-si	−2.65	17.15	19.80	−17.72
Anti-re	−2.50	17.71	20.21	−18.04

[a] Total ZPE corrected energies (electronic + ZPE in a.u.) of active catalysts and olefin are: $[p\text{-OMe-MBz}...TiCl_2CH_3]^+ = -2384.106503$; $C_3H_6 = -117.827460$. *p*-OMe-MBz = *para*-methoxy methyl benzoate internal additive. ZPEs used are without scaling.
[b] E_{act} is insertion barrier in kcal/mol.

Ti–alkyl bond in the *syn*-and *anti*-structures leads to the formation of anti-Markovnikov (Ti bonded to unsubstituted or less branched carbon) and Markovnikov products, respectively. Since propylene is a prochiral molecule, in each of these structures there are two further possibilities according to coordination of propylene to titanium center by two different enantiofaces. These are referred to by suffix *si* and *re* according to the *si* and *re* faces of propylene facing the Ti–C(alkyl) bond. More precisely *si* and *re* refer to structures, where the methyl group of propylene is above or below the plane formed by Ti and the two C atoms of the double bond in propylene, respectively (cf. Scheme 1).

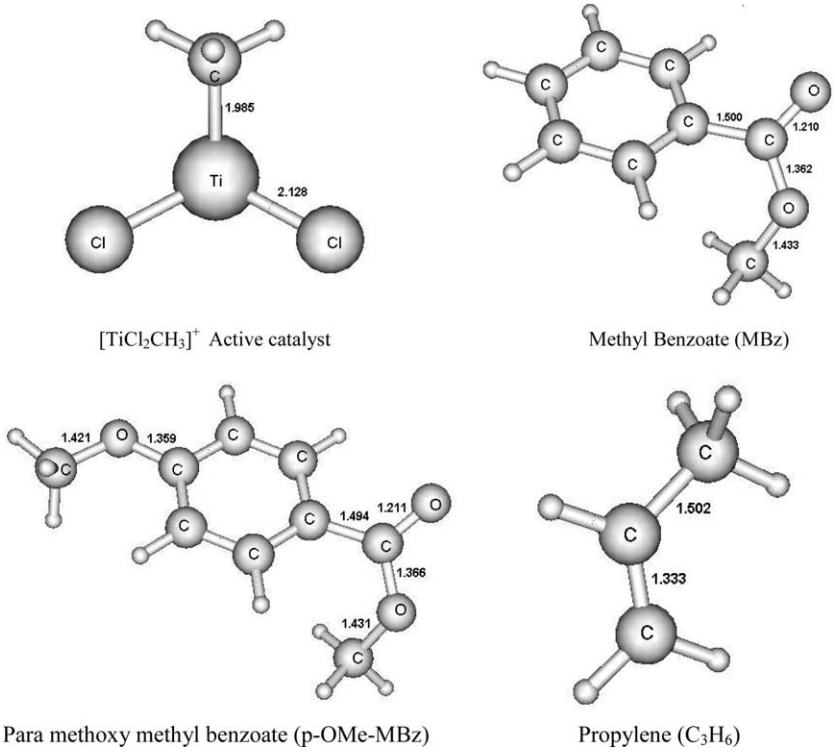

$[TiCl_2CH_3]^+$ Active catalyst
Methyl Benzoate (MBz)
Para methoxy methyl benzoate (p-OMe-MBz)
Propylene (C_3H_6)

Fig. 1. Optimized geometries of stationary points observed for $[TiCl_2CH_3]^+$ active catalyst, propylene and methyl benzoate, *para*-methoxy methyl benzoate as internal additives at B3LYP/6-31G* level. Bond lengths are in Å. All the structures have been visualized by using MDS molecular modeling software [11].

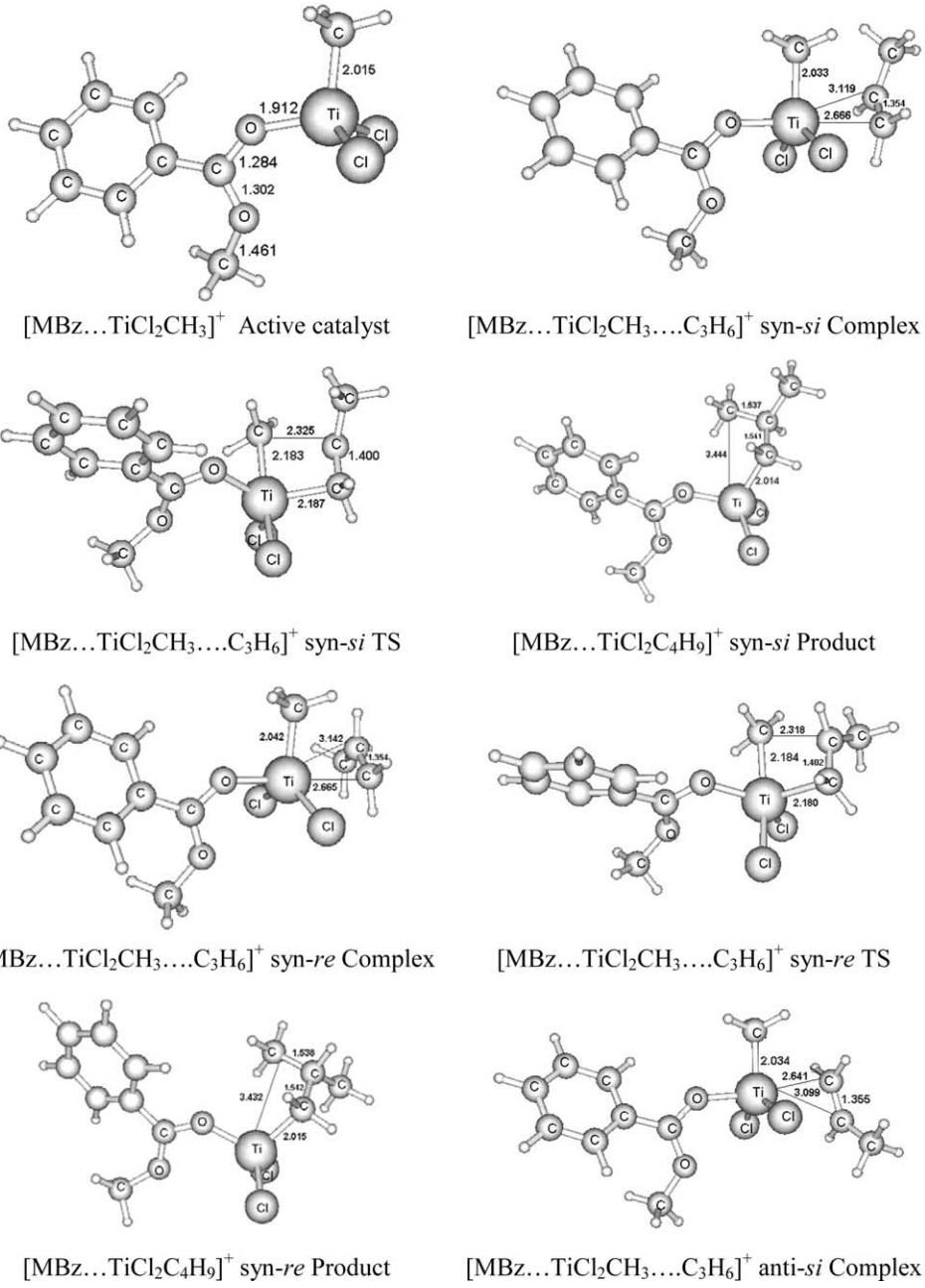

Fig. 2. Optimized geometries of stationary points observed for propylene insertion in $[MBz\ldots TiCl_2CH_3]^+$ active catalyst at B3LYP/6-31G* level. Bond lengths are in Å.

The active catalysts, and the products of first propylene insertion in the Ti–CH_3 bond, have pseudo tetrahedral geometries (cf. Figs. 2 and 4). The tetrahedral Ti in the active catalyst has the fifth coordination site open to accept an incoming propylene molecule. The propylene complexes and the transition states for the insertion of propylene into the Ti–CH_3 bond, have pseudo trigonal bipyramidal (TBP) geometry around the Ti center (cf. Figs. 2 and 4).

In the TBP geometry of the complexes and the transition states, the methyl and the two chloride ligands lie in the equatorial plane (cf. Figs. 2 and 4). Propylene and the electron donor (MBz or *p*-OMe-MBz) occupy axial positions. In all the stationary points the coordination of the electron donor to titanium takes place through the carbonyl oxygen of the ester functionality. It may be noted that single crystal X-ray structure of diester adducts of $TiCl_4$ has been reported in the literature [10]. The computed structures where monoesters are found to co-ordinate to $TiCl_4$ through the carbonyl oxygen atoms are in accordance with these reported structures.

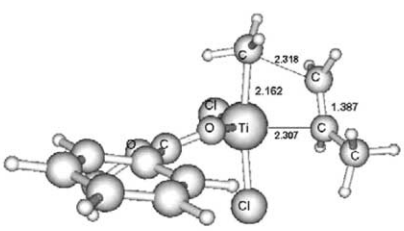

$[MBz\ldots TiCl_2CH_3\ldots.C_3H_6]^+$ anti-*si* TS

$[MBz\ldots TiCl_2C_4H_9]^+$ anti-*si* Product

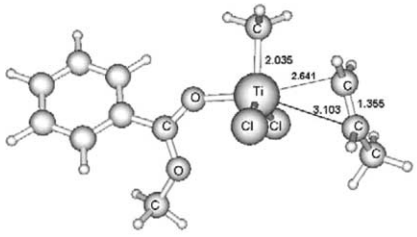

$[MBz\ldots TiCl_2CH_3\ldots.C_3H_6]^+$ anti-*re* Complex

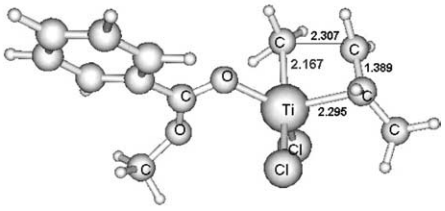

$[MBz\ldots TiCl_2CH_3\ldots.C_3H_6]^+$ anti-*re* TS

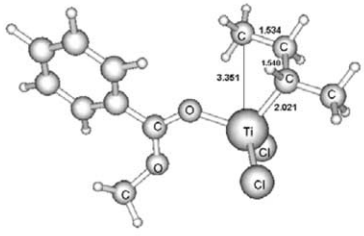

$[MBz\ldots TiCl_2C_4H_9]^+$ anti-*re* Product

Fig. 2 (*continued*)

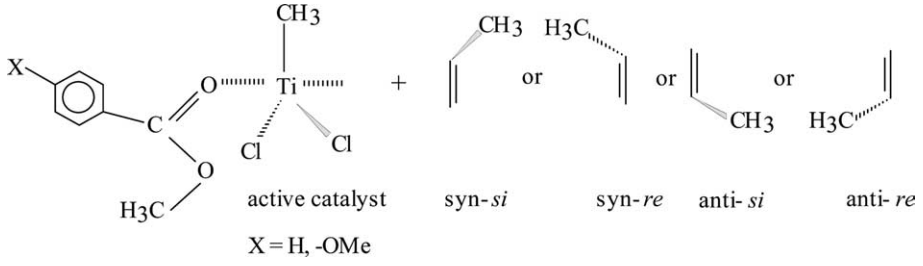

Scheme 1.

3.1. Structure and bonding aspects

The optimized geometries of the active catalyst $[MBz\ldots TiCl_2CH_3]^+$, the catalytic intermediates with co-ordinated propylene, the TSs for propylene insertion into the Ti–CH_3 bond, and the final products are shown in Fig. 2. The corresponding relative energy profile is also shown in Fig. 3.

In the active catalyst $[MBz\ldots TiCl_2CH_3]^+$ the Ti–O bond distance is 1.912 Å. The Ti–O bond elongates by about 0.06 Å in the *syn* and *anti* propylene complexes, by about 0.12 Å in the corresponding TSs, and reduces to around 1.933 Å in the final products. This is a reflection of the change of coordination number from four (active catalyst) to five (complexes and transition states) and again to four (products).

The Ti–CH_3 bond elongates from 2.015 Å in active catalyst to 2.033 Å in *syn-si*, 2.042 Å in *syn-re*, 2.034 Å in *anti-si*, 2.035 Å in *anti-re* complexes. It further increases to 2.183 Å, 2.184 Å in *syn-si*, *syn-re* and 2.162 Å, 2.167 Å in *anti-si*, *anti-re* transition states(TSs), respectively. This indicates progressive weakening of the Ti–CH_3 bond as the active catalyst is converted first to the propylene complex and then to the TS. It should

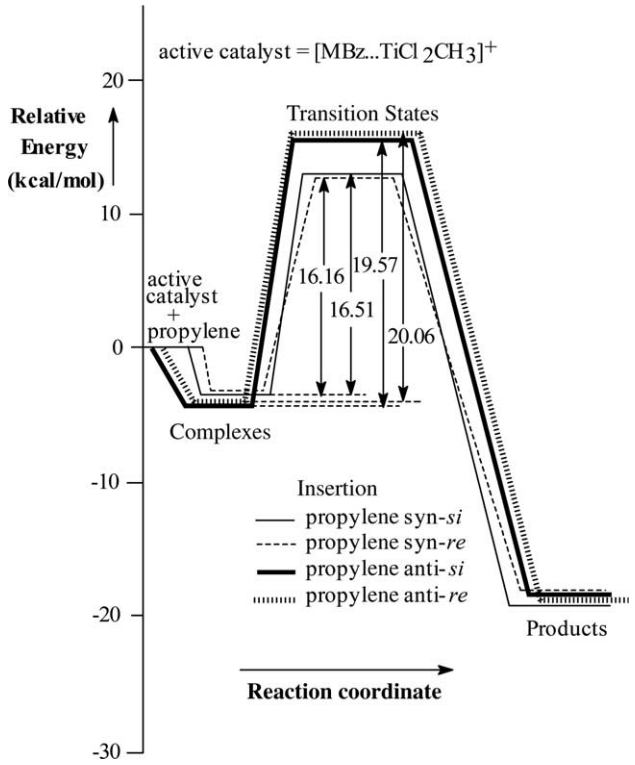

Fig. 3. Relative energy profile for propylene insertion into $[MBz...TiCl_2CH_3]^+$ at B3LYP/6-31G* level after inclusion of zero point energy correction.

be noted that the Ti–CH_3 bonds are longer in case of *syn* TS than the corresponding *anti*. The Ti–CH_3 bond eventually breaks during the insertion reaction and the products with growing alkyl chain are formed (cf. Fig. 2).

In *syn-si* and *syn-re* complexes the propylene molecule is almost perpendicular to the Ti–CH_3 bond. In the TSs it is oriented almost parallel to the Ti–CH_3 bond. In propylene complexes, the shorter of the two Ti–C(propylene) distances are 2.666, 2.665, 2.641 and 2.641 Å in *syn-si*, *syn-re*, *anti-si* and *anti-re* complexes, respectively. It should be noted that there is a greater elongation of C=C bond from *syn* complex to *syn* TS than in the corresponding *anti* complex to *anti* TS.

The optimized geometries for complexes, TSs and products for propylene insertion into Ti–CH_3 bond of active catalyst $[p\text{-OMe-MBz}...TiCl_2CH_3]^+$ are shown in Fig. 4 and corresponding relative energy profile is displayed in Fig. 5. In the four coordinated active catalyst $[p\text{-OMe-MBz}...TiCl_2CH_3]^+$ the Ti–O bond distance is 1.894 Å which is shorter than that in $[MBz...TiCl_2CH_3]^+$. The trends in variation of Ti–O and Ti–CH_3 bonds from $[p\text{-OMe-MBz}...TiCl_2CH_3]^+$ to corresponding *syn* and *anti* propylene complexes, TSs and products are similar to those in the $[MBz...TiCl_2CH_3]^+$ system. The overall structural and bonding features in the *p*-OMe-MBz catalytic complexes, TSs and products are also similar (cf. Fig. 4) to those for the MBz catalyst and therefore are not discussed in detail.

3.2. Energetics

The ZPE corrected relative energies (kcal/mol) for propylene insertion reactions using $[TiCl_2CH_3]^+$ as model catalyst and methyl benzoate and *p*-OMe methyl benzoate as internal additives at B3LYP/6-31G* level are shown in Tables 1 and 2, respectively and the corresponding relative energy profiles are shown in Figs. 3 and 5, respectively. The energies reported in Tables 1 and 2 are relative to energies of the two reactants, i.e., active catalysts and propylene and the activation barriers (E_{act}) refer to insertion of propylene in the Ti–CH_3 bond. The relative energy values (kcal/mol) in parentheses in Table 1 are for the corresponding single point energies at B3LYP/ 6-311+G(d,p) level of calculation. In the following discussion unless otherwise explicitly mentioned, the relative energy values discussed are the ZPE corrected values (not in parentheses in Table 1) at B3LYP/6-31G* level.

Co-ordination by MBz or *p*-OMe-MBz to $[TiCl_2Me]^+$ results in complexes in which the latter is stabilized more by 6.18 kcal/mol than $[MBz...TiCl_2CH_3]^+$ complex. These complexes are the active catalysts for propylene polymerization in the present study. The results in Table 1 and 2 show that the individual propylene π-complex stabilization energies (E(Complex)) for the complexes with MBz as the electron donor are lower than that for the corresponding complexes with *p*-OMe-MBz as the electron donor. This may be rationalized in terms of the donor ability of the methoxy substituent in *p*-OMe-MBz. The positive charge on Ti is partly quenched due to the extra donation, which probably leads to lower stabilization energy. This fact is also reflected in the Ti–O distances in the corresponding catalysts which show shorter Ti–O bond in $[p\text{-OMe-MBz}...TiCl_2CH_3]^+$ compared to that in $[MBz...TiCl_2CH_3]^+$ as discussed earlier in Section 3.1 (cf. Figs. 2 and 4).

The activation barriers for $[MBz...TiCl_2CH_3...C_3H_6]^+$ complexes are 16.51 (*syn-si*) and 16.16 (*syn-re*), 19.57 (*anti-si*) and 20.06 (*anti-re*) kcal/mol (cf. Table 1). The propylene insertion in $[p\text{-OMe-MBz}...TiCl_2CH_3...C_3H_6]^+$ complexes have activation barriers of 16.65 (*syn-si*), 16.41 (*syn-re*), 19.80 (*anti-si*) and 20.21 (*anti-re*) kcal/mol (cf. Table 2). These results indicate that the activation barriers (E_{act}) of corresponding structures of MBz and *p*-OMe-MBz are not significantly different.

In order to study the effect of basis set on the trends of relative energies, we have also performed single point calculations at the above optimized geometries using 6-311++G(d,p) basis set for the MBz catalyst system. The trends in the relative energies are similar for *syn* and *anti* complexes, their corresponding activation barriers (E_{act}) and products at both levels of calculation (cf. Table 1). The overall trend of relative energies of *anti* TSs being higher than the *syn* TSs is reproduced at both levels of calculations. Similar

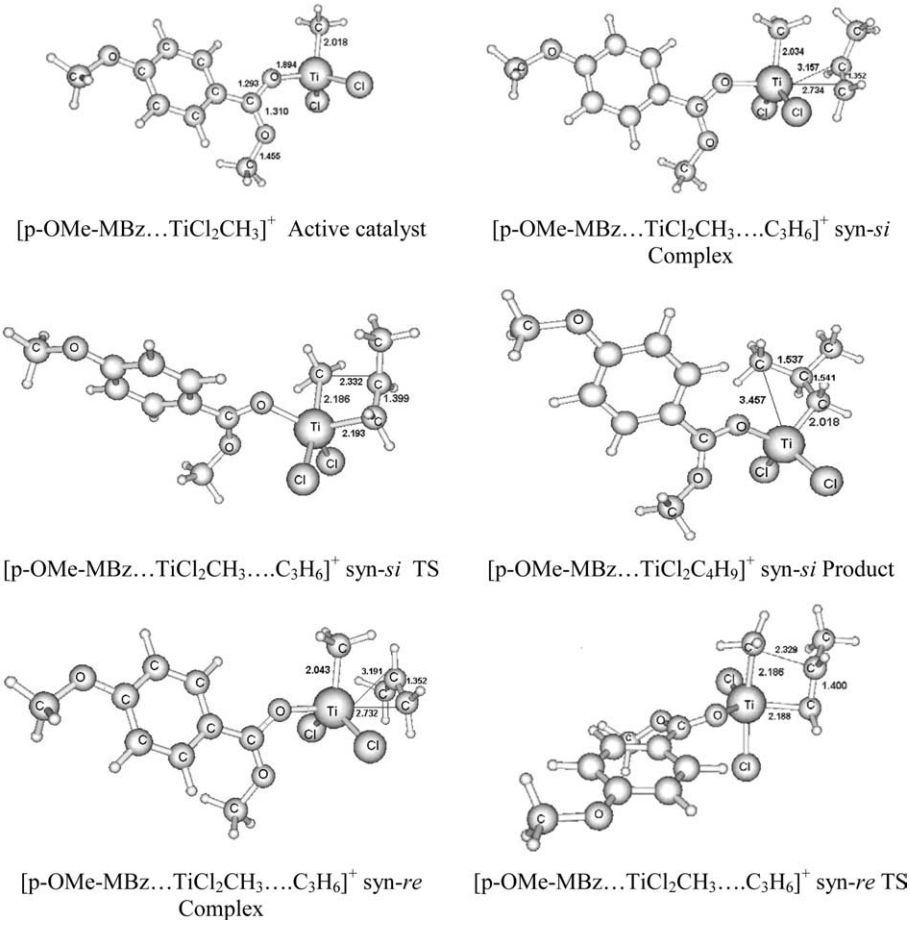

Fig. 4. Optimized geometries of stationary points observed for propylene insertion in [*p*-OMe-MBz. . .$TiCl_2CH_3$]$^+$ active catalyst at B3LYP/6-31G* level. Bond lengths are in Å.

trends are also expected for propylene insertion in [*p*-OMe-MBz. . .$TiCl_2CH_3$. . .C_3H_6]$^+$ at the higher level basis set, 6-311++G(d,p).

From the activation barriers it is clear that for both the electron donors, propylene insertion in *anti* fashion requires more than 3 kcal/mol of extra activation energy than in *syn* fashion. This fact is also reflected in the Ti–CH_3 distances in the corresponding catalysts which show longer Ti–CH_3 bond in case of *syn* TS than the corresponding *anti* TS. Further, greater elongation of C=C bond from *syn* complex to *syn* TS than from *anti* complex to *anti* TS for both [*p*-OMe-MBz . . .$TiCl_2CH_3$. . .C_3H_6]$^+$ and [MBz. . .$TiCl_2CH_3$. . .C_3H_6]$^+$ systems (cf. Figs. 2 and 4) are observed. Similar trends, i.e., less activation barriers for *syn* insertions in propylene complexes of the type [$TiCl_2(CH_3)$]$^+$ and [Ti-Cl(OR)(CH_3)]$^+$ were also seen in our previous works [7a]. The preference for *syn* insertion is in accordance with the general experimental observation, that in propylene polymerization with commercial ZN catalysts *syn*(1,2) insertion (anti-Markovnikov) is the preferred mode [6c,d]. The preference for *syn* insertion is probably steric in nature and has been reported by other workers for propylene polymerization with both the regioselectivity, stereospecificity preferences [6c,d].

At B3LYP/6-31G* level of calculation, the activation barrier for *syn* propylene insertion in the Ti–CH_3 bond of the active catalyst [$TiCl_2Me$]$^+$ is 11.63 kcal/mol. With [MBz. . .$TiCl_2CH_3$]$^+$ and [*p*-OMe-MBz. . .$TiCl_2CH_3$]$^+$ as the active catalysts, the activation barriers (E_{act}) of *syn* insertion of propylene in the Ti–CH_3 bond lie within the range of 16.16–16.65 kcal/mol (cf. Tables 1 and 2). Thus, the insertion barriers in the presence of internal additives are significantly higher (by 4.5–5.0 kcal/mol) than that for the corresponding [$TiCl_2Me$]$^+$ catalyst. The rates of polymerization in the presence of the electron donors are thus expected to be lower. Assuming that the pre-exponential factor remains constant, the rate constants in the presence of the electron donors are expected to be more than three orders of magnitude less than that in their absence. From data available in the literature, a commercial catalyst with ethyl benzoate as the electron donor is about 20–25% less active than the one without an electron donor [2b]. In a multi-site solid catalyst the contribution of a given type of active site is expected to be limited, and that of a tri-coordinate

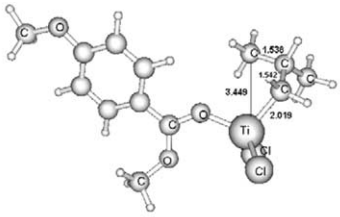

[p-OMe-MBz…$TiCl_2C_4H_9$]$^+$ syn-*re* Product

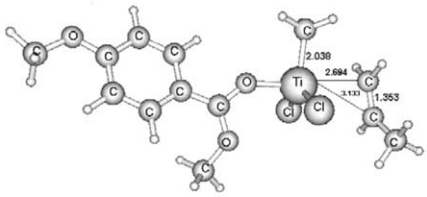

[p-OMe-MBz…$TiCl_2CH_3$….C_3H_6]$^+$ anti-*si* Complex

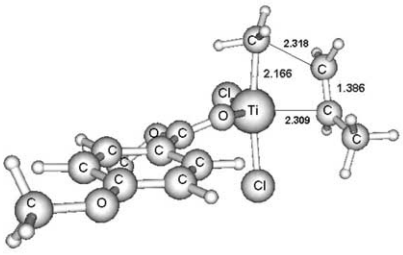

[p-OMe-MBz…$TiCl_2CH_3$….C_3H_6]$^+$ anti-*si* TS

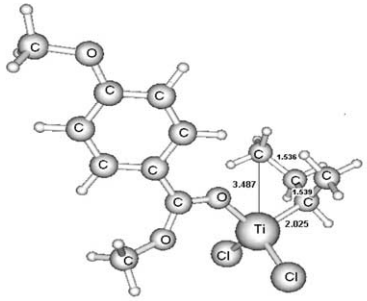

[p-OMe-MBz…$TiCl_2C_4H_9$]$^+$ anti-*si* Product

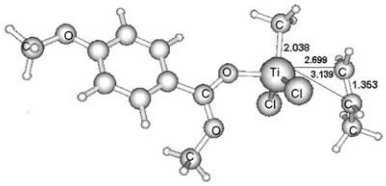

[p-OMe-MBz…$TiCl_2CH_3$….C_3H_6]$^+$ anti-*re* Complex

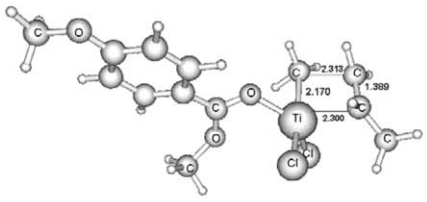

[p-OMe-MBz…$TiCl_2CH_3$….C_3H_6]$^+$ anti-*re* TS

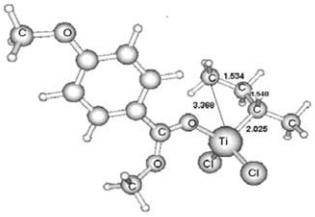

[p-OMe-MBz…$TiCl_2C_4H_9$]$^+$ anti-*re* Product

Fig. 4 (*continued*)

active site approximating $[TiCl_2Me]^+$ is expected to be very small [6l]. This probably explains why on addition of the electron donor a small, rather than orders of magnitude drop in activity is observed.

An analysis of the relative stabilization energies of the individual π-complexes reveals the following interesting observation. The propylene π-complex stabilization energies (*E*(Complex)) for the complexes with MBz and *p*-OMe-MBz as electron donors range from −3.28 to −4.01 and −1.92 to −2.65 kcal/mol, respectively (cf. Tables 1 and 2). The corresponding stabilization energies in the absence of electron donors are typically −44.7 kcal/mol. Thus, on co-ordination by the electron donors there is almost an order of magnitude decrease in the stabilization energies. This could be rationalized on the basis of higher availability of positive charge on Ti in $[TiCl_2Me]^+$ for interaction with propylene, than on Ti in $[MBz...TiCl_2CH_3]^+$ and $[p\text{-OMe-MBz}...TiCl_2CH_3]^+$. These results indicate decreased interaction between Ti and propylene on adding the electron donors to $[TiCl_2Me]^+$ which in turn could have some impact on its deactivation.

The energies of propylene insertion reactions, i.e., catalyst…olefin complex → alkyl product, can be computed from the relative stabilization energies of the olefin complex and products of first propylene insertion reported in Tables 1 and 2. These show that propylene insertion reactions are exothermic by about 15 kcal/mol for all the $[MBz...TiCl_2CH_3]^+$ and $[p\text{-OMe-MBz}...TiCl_2CH_3]^+$ systems studied in this work. Whereas propylene insertion into $[TiCl_2Me]^+$ catalyst in *syn* fashion [7a] is endothermic by 3.33 kcal/mol at

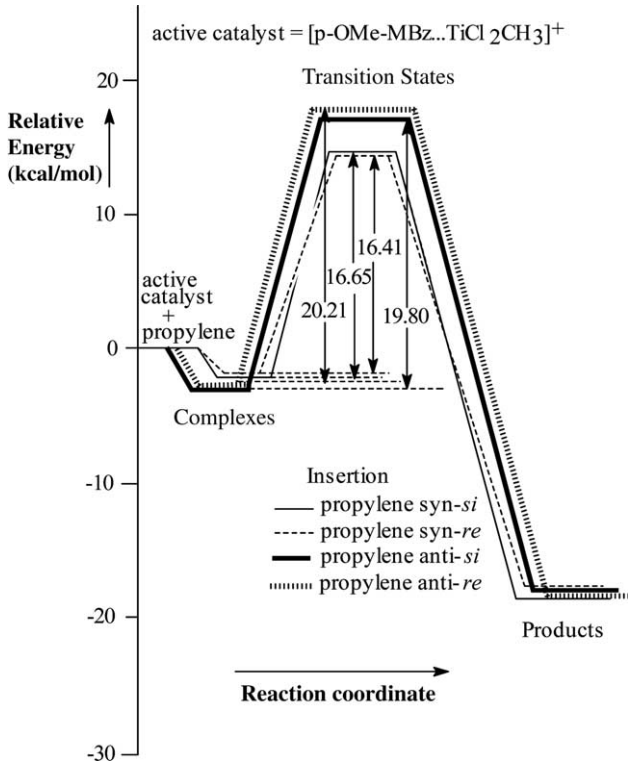

Fig. 5. Relative energy profile for propylene insertion into [*p*-OMe-MBz...$TiCl_2CH_3$]$^+$ at B3LYP/6-31G* level after inclusion of zero point energy correction.

6-31G* level as found in this work. This indicates greater product stabilization for first propylene insertion in the [MBz...$TiCl_2CH_3$]$^+$ and [*p*-OMe-MBz...$TiCl_2CH_3$]$^+$ systems than in [$TiCl_2Me$]$^+$ which could be due to the presence of the internal electron donors in the former two systems.

It may be noted that for both the electron donors, there is a small difference between the activation barriers for propylene insertion of *syn-si* and *syn-re* complexes (cf. Tables 1 and 2). Although one may want to attribute this to a small but observable kinetic preference for propylene insertion in a *stereospecific* manner, it could be an artifact of basis set and level of calculations used.

4. Concluding remarks

The purpose of this study was to find out the role of monoester electron donors on the performance of Ziegler–Natta catalyst in propylene polymerization. To the best of our knowledge, this is the first density functional report of the role of two typical monoester electron donors for this purpose where we could rationalize the regioselective tuning of ZN catalysed propylene polymerization by such donors starting from the simple model catalyst, [$TiCl_2Me$]$^+$.

Our results agree well with two major literature reported experimental observations. Firstly, the regioselectivity (anti-Markovnikov) of propylene insertion is found to be maintained in the presence of electron donors. For both the electron donors, the propylene insertions in *syn* fashion have lower activation barriers (E_{act}) than the corresponding *anti* fashion. Secondly, co-ordination of electron donors is found to increase the activation barriers of propylene insertion, which explains the experimentally observed drop in catalytic activity. We have found that the propylene *syn* insertion barriers in presence of internal additives are significantly higher (by 4.5–5.0 kcal/mol) than that for the corresponding [$TiCl_2Me$]$^+$ catalyst. This is in agreement with the widely reported experimental observation that in the presence of electron donors there is a drop in the catalytic activity of ZN catalysts.

Finally, for both electron donors, there is a small difference between the activation barriers for propylene insertion of *syn-si* and *syn-re* complexes. Though this seems attributable to a small but observable kinetic preference for propylene insertion in a *stereospecific* manner, this could actually be an artifact of basis set and level of calculations used. It is known that the stereospecificity of polypropylene with a ZN catalyst is mainly dependent on the second and subsequent propylene insertion, rather than the first insertion reaction [6d]. Work on other electron donors and second propylene insertion in the [MBz...$TiCl_2C_4H_9$]$^+$ and [*p*-OMe-MBz...$TiCl_2C_4H_9$]$^+$ systems is in progress.

Acknowledgements

Authors are grateful to Professor S.R. Gadre, University of Pune, India and to Dr. Libero Bartolotti, Department of Chemistry, East Carolina University, USA for providing computer facility. Financial support for this work was provided by Reliance Industries Limited. We thank the referees for useful suggestions.

References

[1] W. Kaminsky, J. Chem. Soc. Dalton. Trans. (1998) 1413.
[2] (a) G.G. Arzoumanidis, N.M. Karayannis, Chemtech (July) (1993) 43;
(b) E. Albizzati, U. Giannini, G. Morini, C.A. Smith, R.C. Zeigler, in: G. Fink, R. Mulhaupt, H.H. Brintzinger (Eds.), Ziegler Catalysts, Springer-Verlag, Berlin, 1995, p. 413, and references therein;
(c) J.C. Chadwick, in: G. Fink, R. Mulhaupt, H.H. Brintzinger (Eds.), Ziegler Catalysts, Springer-Verlag, Berlin, 1995, p. 427, and references therein.
[3] G.G. Arzoumanidis, N.M. Karayannis, Appl. Catal. 76 (1991) 221–231.
[4] (a) M. Seth, T. Ziegler, Macromolecules 36 (2003) 6613, and references therein;

(b) M. Boero, M. Parrinello, H. Weiss, S. Huffer, J. Phys. Chem. A 105 (2001) 5096–5105, and references therein;
(c) S.Y. Lim, S.J. Choung, J. Appl. Polymer Sci. 67 (1998) 1779.
[5] (a) B.L. Goodall, J. Chem. Educ. 63 (1986) 191;
(b) P. Sobota, S. Szafert, J. Chem. Soc. Dalton Trans. (2001) 1379, and references therein.
[6] (a) A.K. Rappe, W.M. Skiff, C.J. Casewit, Chem. Rev. 100 (2000) 1435–1456, and references therein;
(b) V.C. Gibson, S.K. Spitzmesser, Chem. Rev. 103 (2003) 283–315, and references therein;
(c) H. Kawamura-Kuribayashi, N. Koga, K. Morokuma, J. Am. Chem. Soc. 114 (1992) 2359–2366;
(d) M. Boero, M. Parrinello, S. Huffer, H. Weiss, J. Am. Chem. Soc. 122 (2000) 501–509, and references therein;
(e) M. Boero, M. Parrinello, K. Terakura, J. Am. Chem. Soc. 120 (1998) 2746;
(f) P. Corradini, V. Busico, G. Guerra, Monoalkene Polymerization: Stereospecificity in Comprehensive Polymer Science, 4, 1988, pp. 29–50;
(g) V. Busico, R. Cipullo, P. Corradini, R. De Biasio, Macromol. Chem. Phys. 196 (1995) 491;
(h) L. Cavallo, G. Guerra, P. Corradini, J. Am. Chem. Soc. 120 (1998) 2428;
(i) G. Morini, E. Albizzati, G. Balbontin, I. Mignozzi, M.C. Sacchi, F. Forlini, I. Tritto, Macromolecules 29 (1996) 5770;
(j) E. Albizzati, U. Giannini, G. Balbontin, I. Camurati, J.C. Chadwick, T. Dall'Occo, Y. Dubitsky, M. Galimberti, G. Morini, A. Maldotti, J. Polym. Sci.: Polym. Chem. 35 (1997) 2645;
(k) M. Toto, G. Morini, G. Guerra, P. Corradini, L. Cavallo, Macromolecules 33 (2000) 1134, and references therein;
(l) M. Seth, P.M. Margl, T. Ziegler, Macromolecules 35 (2002) 7815–7829;
(m) M. Boero, M. Parrinello, K. Terakura, H. Weiss, Mol. Phys. 100 (2002) 2935;
(n) P. Cossee, J. Catal. 3 (1964) 65;
(o) E.J. Arlman, P. Cossee, J. Catal. 3 (1964) 80, 89, 99.
[7] (a) S. Bhaduri, S. Mukhopadhyay, S.A. Kulkarni, J. Organomet. Chem. 671 (2003) 101–112;
(b) S. Mukhopadhyay, S.A. Kulkarni, S. Bhaduri, J. Mol. Struct. (Theochem.) 673 (2004) 65–77.
[8] (a) A.D. Becke, Phys. Rev. A 38 (1988) 3098;
(b) C. Lee, W. Yang, R.G. Parr, Phys. Rev. B 37 (1988) 785;
(c) A.D. Becke, J. Chem. Phys. 98 (1993) 5648.
[9] M.J. Frisch, G.W. Trucks, H.B. Schlegel, G.E. Scuseria, M.A. Robb, J.R. Cheeseman, V.G. Zakrzewski, J.A. Montgomery Jr., R.E. Stratmann, J.C. Burant, S. Dapprich, J.M. Millam, A.D. Daniels, K.N. Kudin, M.C. Strain, O. Farkas, J. Tomasi, V. Barone, M. Cossi, R. Cammi, B. Mennucci, C. Pomelli, C. Adamo, S. Clifford, J. Ochterski, G.A. Petersson, P.Y. Ayala, Q. Cui, K. Morokuma, P. Salvador, J.J. Dannenberg, D.K. Malick, A.D. Rabuck, K. Raghavachari, J.B. Foresman, J. Cioslowski, J.V. Ortiz, A.G. Baboul, B.B. Stefanov, G. Liu, A. Liashenko, P. Piskorz, I. Komaromi, R. Gomperts, R.L. Martin, D.J. Fox, T. Keith, M.A. Al-Laham, C.Y. Peng, A. Nanayakkara, M. Challacombe, P.M.W. Gill, B. Johnson, W. Chen, M.W. Wong, J.L. Andres, C. Gonzalez, M. Head-Gordon, E.S. Replogle, J.A. Pople, GAUSSIAN 98, Revision A.11, Gaussian, Inc., Pittsburgh PA, 2001.
[10] P. Sobota, S. Szafert, T. Lis, J. Organomet. Chem. 443 (1993) 85.
[11] MDS 2.0: Molecular Design Suite, VLife Sciences Technologies Pvt. Ltd., Pune, India, 2004.